June 1994

Model-based Analysis of Cardiac Motion from Tagged MRI Data

Jinah Park
University of Pennsylvania

Dimitris Metaxas
University of Pennsylvania

Alistair A. Young
University of Pennsylvania

Leon Axel
University of Pennsylvania, axel@oasis.rad.upenn.edu

Model-based Analysis of Cardiac Motion from Tagged MRI Data

Abstract
We develop a new method for analyzing the motion of the left ventricle (LV) of a heart from tagged MRI data. Our technique is based on the development of a new class of physics-based deformable models whose parameters are functions allowing the definition of new parameterized primitives and parameterized deformations. These parameter functions improve the accuracy of shape description through the use of a few intuitive parameters such as functional twisting. Furthermore, these parameters require no complex post-processing in order to be used by a physician. Using a physics-based approach, we convert these geometric models into deformable models that deform due to forces exerted from the datapoints and conform to the given dataset. We present experiments involving the extraction of shape and motion of the LV from MRI-SPAMM data based on a few parameter functions. Furthermore, by plotting the variations over time of the extracted model parameters from normal and abnormal heart data we are able to characterize quantitatively their differences.

Model-based Analysis of Cardiac Motion from Tagged MRI Data

Jinah Park[1], Dimitri Metaxas[1], Alistair Young[2] and Leon Axel[2]

[1]Department of Computer & Information Science
University of Pennsylvania
Philadelphia PA 19104-6389

[2]Department of Radiology
University of Pennsylvania
Philadelphia PA 19104

Abstract

We develop a new method for analyzing the motion of the left ventricle (LV) of a heart from tagged MRI data. Our technique is based on the development of a new class of physics-based deformable models whose parameters are functions allowing the definition of new parameterized primitives and parameterized deformations. These parameter functions improve the accuracy of shape description through the use of a few intuitive parameters such as functional twisting. Furthermore, these parameters require no complex post-processing in order to be used by a physician. Using a physics-based approach, we convert these geometric models into deformable models that deform due to forces exerted from the datapoints and conform to the given dataset. We present experiments involving the extraction of shape and motion of the LV from MRI-SPAMM data based on a few parameter functions. Furthermore, by plotting the variations over time of the extracted model parameters from normal and abnormal heart data we are able to characterize quantitatively their differences.

1 Introduction

Characterization of heart wall motion on a regional level is required to understand cardiac mechanics and the processes underlying disease. Alteration of heart wall motion is a sensitive indicator of disease such as ischemia. In order to accurately measure heart wall motion a number of material points must be located and tracked. One of the methods for providing markers is by using the magnetic resonance imaging (MRI) technique with magnetic tagging ("SPAMM") [2, 12]. The advantage of MR tagging is that a number of material points can be tracked during systole in a non-invasive setting, providing temporal correspondence of material points.

Recently, computer vision techniques for reconstructing the 3D shape and motion of the heart's left ventricle (LV) have been developed [1, 3, 4, 6, 8, 9, 11]. One problem with the techniques developed so far is that they do not capture the twisting motion of the heart, known to occur during systole. Also, they are formulated in terms of either many local parameters that require non-trivial processing to be useful to a physician, or very few parameters that can offer only a gross approximation of the motion.

In this paper we present a new technique that describes the time-varying shape, deformation and shape of the LV in terms of a few "global" *parameter functions*, such as twist, whose value is allowed to vary locally. In this way, we can characterize the complex motion of the heart in terms of the same small number of parameters that offer sufficient accuracy. Furthermore, these parameters are intuitive and can be used by a physician without further complex processing. Our approach is based on the development of a new family of parameterized deformable primitives suitable for

1063-7125/94 $3.00 © 1994 IEEE

this application. These deformable primitives are parameterized using parameter functions whose value varies across the primitive's shape as opposed to being constant [7, 10]. Through the use of appropriate parameterization the axes of our new deformable primitives can be curved. This is a major generalization compared to parameterized primitives such as superquadrics, cylinders and cubes, commonly used in the vision literature. Finally, our new models can represent open[1] parameterized shapes suitable for modeling the shape and motion of the LV.

2 Geometry of Deformable Models with Parameter Functions

In this section we introduce our new class of deformable models which allows the use of parameters that can characterize an object's shape in terms of a few parameters that are functions. In general, our model is a 3D surface whose material coordinates $\mathbf{u} = (u, v)$ are defined in a domain Ω. The positions of points on the model relative to an inertial frame of reference Φ in space are given by a vector-valued, time varying function $\mathbf{x}(\mathbf{u}, t) = (x_1(\mathbf{u}, t), x_2(\mathbf{u}, t), x_3(\mathbf{u}, t))^\top$, where $^\top$ denotes transposition. We set up a non-inertial, model-centered reference frame ϕ and express the position of a model point as $\mathbf{x} = \mathbf{c} + \mathbf{R}\mathbf{s}$, where $\mathbf{c}(t)$ is the origin of ϕ at the center of the model and the rotation matrix $\mathbf{R}(t)$ gives the orientation of ϕ relative to Φ with a reference shape $\mathbf{s}$. Thus, $\mathbf{s}(\mathbf{u}, t)$ gives the positions of points on the model relative to the model frame.

We define the reference shape as $\mathbf{s} = \mathbf{T}(\mathbf{e}; b_0(\mathbf{u}), b_1(\mathbf{u}), \ldots)$, where $\mathbf{e}$ can represent either a set of 3D points in space[2] or a geometric primitive $\mathbf{e}(\mathbf{u}; a_0(\mathbf{u}), a_1(\mathbf{u}), \ldots)$ defined parametrically in $\mathbf{u}$ and parameterized by the variables $a_i(\mathbf{u})$. The shape represented by $\mathbf{e}$ is subjected to the *deformation* $\mathbf{T}$ which depends on the deformation parameter functions $b_i(\mathbf{u})$. We concatenate the deformation parameters into the vector $\mathbf{q}_s = (a_0(\mathbf{u}), a_1(\mathbf{u}), \ldots, b_0(\mathbf{u}), b_1(\mathbf{u}), \ldots)^\top$.

The parameters a_i and b_i are functions of $\mathbf{u}$, instead of constants [7]. This definition allows us to generalize definitions of primitives (e.g., superquadrics, cubes) and parameterized deformations (e.g., twisting) as will be shown in the following example. For our applications, we will assume that $a_i(\mathbf{u}) = a_i(u)$, $b_i(\mathbf{u}) = b_i(u)$, where the material coordinate u corresponds to the longest axis of the deformable model.

Our technique for creating primitives with parameter functions can be applied to any parametric primitive, by replacing its constant parameters with differentiable parameter functions. For our applications, we transform an ellipsoid primitive [7] to a primitive with parameter functions. The definition of such a generalized primitive $\mathbf{e} = (e_1, e_2, e_3)^\top$ is given as follows:

$$\mathbf{e} = a_0 \begin{pmatrix} a_1(u) \cos u \cos v \\ a_2(u) \cos u \sin v \\ a_3(u) \sin u \end{pmatrix}, \tag{1}$$

where $-\pi/2 \leq u \leq \pi/2$, $-\pi \leq v < \pi$. Here, $a_0 \geq 0$ is a scale parameter, and $0 \leq a_1(u), a_2(u), a_3(u) \leq 1$, are aspect ratio parameter functions. We can also define a open parameterized primitive given by the above definition by restricting the ranges of the u and v parameters to a subset of the above definition.

Our formulation of deformations with continuous parameter functions is general and can be applied to any underlying shape $\mathbf{e}$. For our applications, given the primitive $\mathbf{e}$, we first apply a twisting deformation along the principal axis 3 (or model axis z), and then apply axis-offset deformations which allow the axis to be non-straight in the x and y directions. In this way we can

[1] not a closed surface, but more like a cup

[2] In that case the material coordinates $\mathbf{u}$ coincide with the cartesian space in which the 3D points are expressed.

recover more accurately the LV shape. The resulting reference shape s is expressed as follows:

$$\mathbf{s} = \mathbf{T}_o(\mathbf{T}_\tau(\mathbf{e}; \tau(u)); e_{1_o}(u), e_{2_o}(u)) = \begin{pmatrix} e_1 \cos(\tau(u)) - e_2 \sin(\tau(u)) + e_{1_o}(u) \\ e_1 \sin(\tau(u)) + e_2 \cos(\tau(u)) + e_{2_o}(u) \\ e_3 \end{pmatrix}, \quad (2)$$

where $\tau(u)$ is the twisting parameter function, and $e_{1_o}(u)$ and $e_{2_o}(u)$ are axis-offset parameter functions in the x and y directions, respectively.

The choice of the parameter functions depends on the application. For the applications in this paper we assume that those parameter functions are piecewise linear along u, so we do not impose any other constraints on the LV shape.

3 Kinematics and Dynamics

The velocity of points on the model is given by, $\dot{\mathbf{x}} = \mathbf{L}\dot{\mathbf{q}}$, where $\mathbf{L}$ is the Jacobian matrix which maps 3D vectors to the model's parameter space and $\mathbf{q} = (\mathbf{q}_c^\top, \mathbf{q}_\theta^\top, \mathbf{q}_s^\top)^\top$ is the vector of the model's degrees of freedom. $\mathbf{q}_c = \mathbf{c}$ and $\mathbf{q}_\theta$ is the vector of the model's rotational parameters. We can make our model dynamic in $\mathbf{q}$ by introducing mass, damping, and a deformation strain energy. The resulting Lagrange equations of motion simplified by setting the mass density to zero are $\mathbf{D}\dot{\mathbf{q}} + \mathbf{K}\mathbf{q} = \mathbf{f}_q$, where $\mathbf{D}$ and $\mathbf{K}$ are the damping and stiffness matrices respectively, and where $\mathbf{f}_q(\mathrm{u}, t)$ are the generalized external forces associated with the degrees of freedom of the model. This equation yields a model that has no inertia and comes to rest when all the applied forces equilibrate or vanish. The generalized forces $\mathbf{f}_q$ are computed using the formula $\mathbf{f}_q = \int \mathbf{L}^\top \mathbf{f}\, d\mathrm{u}$. These forces are associated with the components of $\mathbf{q}$, where $\mathbf{f}(\mathrm{u}, t)$ is the 3D force distribution applied to the model [7].

Since the SPAMM data provides correspondence over time of individual 3D points, we apply the force distribution algorithm only once for the initial frame. In subsequent frames the corresponding points will exert a force to the same point on the model as computed in the first frame. In this way we can recover the LV twisting motion.

4 Experiments

We apply our technique to SPAMM data sequences from a normal heart and an abnormal heart with hypertrophic cardiomyopathy. The data are obtained from the Department of Radiology, University of Pennsylvania collected during the LV systole over 5 intervals. The SPAMM technique provides data throughout the heart wall. However, since our modeling technique is surface based, we choose to fit the LV mid-wall motion since this is most accurately defined by the SPAMM imaging technique. Young *et al.* [11] developed a technique based on snakes [5] to extract 3D coordinates of SPAMM data from the LV mid-wall. In each case we fit our deformable models to the LV mid-wall data points, and plot the time and space varying parameter functions to extract conclusions. All our experiments run at real or interactive time speeds on a Silicon Graphics R4000 Crimson workstation including the real time graphics. Furthermore, through careful design, large portions of our code have been parallelized making it even faster when multiple processors are available (e.g., on our Silicon Graphics 4D/340VGX shared memory multiprocessor).

Fig. 1 shows the model fitted to data points from a normal heart at 5 time sequences during systole from end-diastole (t=1) to end-systole (t=5). We can observe the contracting motion as well as the twisting motion of the model. In Fig. 2 we plot the extracted model parameter functions over the 5 time frames for the normal heart. Figs. 2(a-b) show the plots of the model's parameter functions $a_1(u)$ and $a_2(u)$, which are associated with its length in the x and y directions,

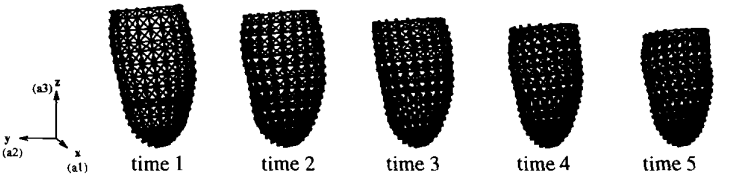

Figure 1: Model fitted to SPAMM data (LV mid-wall) from a normal heart during systole.

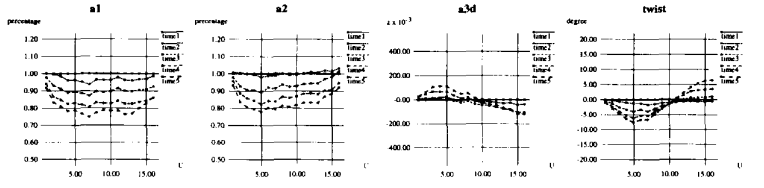

Figure 2: Extracted model parameters as functions of u for the normal heart.

respectively. For each frame we plot the ratio of each parameter function during frame $t = 2...5$, with respect to its value at the initial frame ($t = 1$). Fig. 2(c) shows plots of the displacement[3] of the length along the z direction. Fig. 2(d) shows plots of the model's twisting parameter function $\tau(u)$. In all graphs, $U = 0$ corresponds to u_{min} of the model (the apex of the LV), and $U = 16$ corresponds to u_{max} of the model (the base of the LV).

>From these graphs, we can quantify the motion and shape changes of the LV during its systole. For example, by studying the graphs of a_1 and a_2 (Fig. 2(a-b)), we can conclude that the magnitude of contraction in the radial direction (i.e., along the x and y axes) during systole is approximately 20%. But it is not uniform towards the base of the LV where the contraction along the y axis (being approximately 10%) is less then one along the x axis (being approximately 20%) making the base look more elliptical. This result supports clinical study findings where more stress is exerted at the apex during the LV motion, and also there is an increased closeness to an ellipse of the LV base shape during systole. We measure from the graph shown in Fig. 2(c), that the total displacement along the z axis which corresponds to contraction along the z axis is approximately 0.2 units where the normalized length of the LV is 1.13 units. The contraction along the z axis known as longitudinal contraction is therefore approximately 18% for this LV. From the graph in Fig. 2(d), we can quantify the twisting motion of the LV during systole to approximately 7 degrees. The graph shows a small amount of global rotation before the twisting occurs. It is not easy to see this kind of subtle motion when one watches the model contract and twist on the monitor. By having the graphs of the parameter functions plotted next to the animation, we can quantify and easily characterize a detailed motion of the deforming model over time.

To compare our results, we also fit our model to an abnormal heart with hypertrophic cardiomyopathy. Fig. 3 shows the fitted models for the abnormal heart, while Fig. 4 shows the corresponding graphs of model parameter functions. From the graphs of the parameter functions, we see that they are different from the results we obtained for the normal hearts in Fig. 2. We see

[3]It is not necessary for $a_1(u)$ and $a_2(u)$ because they are not dependent on $\sin u$.

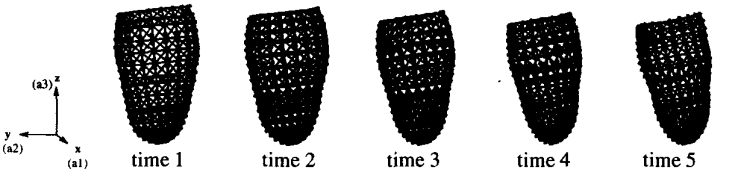

Figure 3: Model fitted to SPAMM data from an abnormal heart during systole.

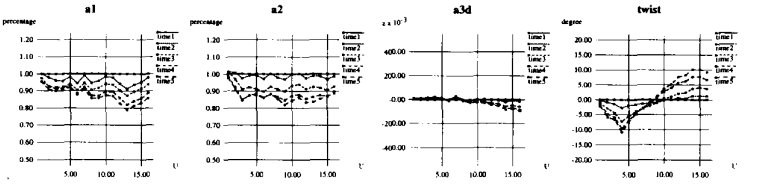

Figure 4: Extracted model parameters as functions of u for the abnormal heart.

less contraction towards the apex of the abnormal heart compared to the normal heart, and more twisting in the abnormal hearts.

In order to view the changes in the parameters during systole, we can shade the meshes of a model with respect to a certain parameter as shown in Fig. 5. The figures in the first row are the recovered models from the normal heart data at different time frames, and the figures in the second row are the recovered models from the abnormal heart data. Figs. 5(a-b) are the models at the initial frame. As the change in value increases, the shading in the corresponding part of the mesh becomes darker. Figs. 5(c-f) and Figs. 5(g-j) show the models color-coded according to the values of the $a_1(u)$ parameters and the values of the $\tau(u)$ parameters, respectively. It can be easily observed that, compared to the normal heart, the abnormal heart has less radial contraction at the end of systole (i.e., the mesh shown in (f) is lighter than one in (e)), but more twisting motion (i.e., the mesh shown in (j) is darker than one in (i)).

Note that all fittings of models are within an acceptable error bound, since RMS errors are less than 0.5 mm where the length of the hearts are approximately 110 mm. Using parameter functions, our model provides the means for capturing and quantifying the LV motion and shape changes. Therefore we can quantitatively compare normal and abnormal hearts.

5 Conclusion

In this paper we presented a new class of physics-based deformable models that can be used to analyze the motion of the LV from tagged MRI data. The characteristic of those models is that their global parameters are functions allowing the representation of complex shapes with a few intuitive parameters. For the applications in this paper we were able to eliminate many local parameters that require nontrivial processing to provide a compact representation of shape. We demonstrated the applicability of our technique to the shape and motion analysis of the LV for normal and abnormal hearts during systole, from MRI-SPAMM data. By plotting the parameter functions over time we were able to make comparisons between normal and abnormal hearts and verify quantitatively, qualitative knowledge about the LV motion common to physicians. We

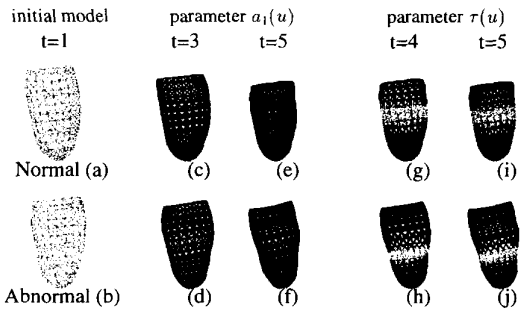

Figure 5: Visualizing changes of values in parameter functions. (Darker drawn areas indicate greater deviation from the initial state.)

plan to apply our technique to multiple normal and abnormal hearts to be able to quantitatively characterize what is normal LV motion and what are the effects to the LV motion of the various LV diseases.

Acknowledgements

We would like to thank Dr. Ken Fellows, the director of the department of Radiology at the Children's Hospital of Philadelphia for his support for the project. The second author was supported by an NSF IRI-9309917 grant.

References

[1] A. Amini and J. Duncan. "Pointwise tracking of Left-Ventricular Motion in 3D," Proc. IEEE Workshop on Visual Motion, pp. 294-298, Princeton, NJ, 1991.

[2] L. Axel, L. Dougherty, "Heartwall motion: Improved method of spatial modulation of magnetization for MR imaging," *Radiology*, **172**, pp. 349-350, 1989.

[3] L. D. Cohen and I. Cohen. "A Finite Element Method Applied to New Active Contour Models and 3D Reconstruction from Cross Sections", Proc. 2nd ICCV, pp. 587-591, Japan 1990.

[4] W-C. Huang and D. Goldgof. Adaptive-Size Meshes for Rigid and Nonrigid Shape Analysis and Synthesis. IEEE Transactions on Pattern Analysis, 15(6), pp. 611-616, 1993.

[5] M. Kass, A. Witkin and D. Terzopoulos. "Snakes: Active Contour Models", International Journal of Computer Vision, 1(4), pp. 321-331, 1988.

[6] T. McInerney and D. Terzopoulos. "A Finite Element Model for 3D Shape Reconstruction and Nonrigid Motion Tracking", Proc. 4th International Conference on Computer Vision, pp. 518-523, Berlin, Germany, 1993.

[7] D. Metaxas and D. Terzopoulos. Shape and Nonrigid Motion Estimation Through Physics-Based Synthesis. *IEEE Trans. Pattern Analysis and Machine Intelligence*, 15(6), pp. 569-579 , June, 1993.

[8] C. Moore, W. O'Dell, E. McVeigh, E. Zerhouni, "Calculation of three-dimensional left ventricular strains form biplanar tagged MR images," *J Mag Res Imag* , **2**, pp. 165-175, 1992.

[9] A. Pentland and B. Horowitz. "Recovery of Nonrigid Motion and Structure". IEEE Pattern Analysis and Machine Intelligence, 13(7), pp. 730-742, July 1991.

[10] D.Terzopoulos and D.Metaxas. Dynamic 3D Models with Local and Global Deformations: Deformable Superquadrics. *IEEE Trans. Pattern Analysis and Machine Intelligence*, 13(7):703–714, 1991. See also Proc. Third International Conference on Computer Vision (ICCV'90), pp. 606-615, Osaka, Japan, Dec. 1990.

[11] A.A. Young, P.J. Hunter, B.H. Smaill, "Estimation of epicardial strain using the motions of coronary bifurcations in biplane cineangiography," *IEEE Trans Biomed Eng*, **39**, pp. 526-531, 1992.

[12] E.A. Zerhouni, D.M. Parish, W.J. Rogers, A. Yang, E.P. Shapiro, "Human heart: Tagging with MR imaging - a method for noninvasive assessment of myocardial motion," *Radiology* **169** pp. 59-63, 1988.